Lineage tracing and targeting of IL17RB$^+$ tuft cell-like human colorectal cancer stem cells

Norihiro Goto[a], Akihisa Fukuda[a], Yuichi Yamaga[a], Takaaki Yoshikawa[a], Takahisa Maruno[a], Hisatsugu Maekawa[b,c], Susumu Inamoto[b], Kenji Kawada[b], Yoshiharu Sakai[b], Hiroyuki Miyoshi[c], Makoto Mark Taketo[c], Tsutomu Chiba[d], and Hiroshi Seno[a,1]

[a]Department of Gastroenterology and Hepatology, Kyoto University Graduate School of Medicine, 606-8507 Kyoto, Japan; [b]Department of Surgery, Kyoto University Graduate School of Medicine, 606-8507 Kyoto, Japan; [c]Division of Experimental Therapeutics, Kyoto University Graduate School of Medicine, 606-8507 Kyoto, Japan; and [d]Department of Gastroenterology and Hepatology, Kansai Electric Power Hospital, 553-0003 Osaka, Japan

Edited by Napoleone Ferrara, University of California San Diego, La Jolla, CA, and approved May 16, 2019 (received for review January 7, 2019)

Cancer stem cell (CSC)-specific markers may be potential therapeutic targets. We previously identified that Dclk1, a tuft cell marker, marks tumor stem cells (TSCs) in mouse intestinal adenomas. Based on the analysis of mouse Dclk1$^+$ tumor cells, we aimed to identify a CSC-specific cell surface marker in human colorectal cancers (hCRCs) and validate the therapeutic effect of targeting it. IL17RB was distinctively expressed by Dclk1$^+$ mouse intestinal tumor cells. Using *Il17rb-CreERT2-IRES-EGFP* mice, we show that IL17RB marked intestinal TSCs in an IL13-dependent manner. Tuft cell-like cancer cells were detected in a subset of hCRCs. In these hCRCs, lineage-tracing experiments in CRISPR-Cas9–mediated *IL17RB-CreERT2* knockin organoids and xenograft tumors revealed that IL17RB marks CSCs that expand independently of IL-13. We observed up-regulation of *POU2F3*, a master regulator of tuft cell differentiation, and autonomous tuft cell-like cancer cell differentiation in the hCRCs. Furthermore, long-term ablation of IL17RB-expressing CSCs strongly suppressed the tumor growth in vivo. These findings reveal insights into a CSC-specific marker IL17RB in a subset of hCRCs, and preclinically validate IL17RB$^+$ CSCs as a cancer therapeutic target.

IL17RB | Dclk1 | CRISPR-Cas9 | organoid

Cancer stem cells (CSCs), capable of self-renewal and giving rise to progeny cells in cancers, have attracted attention as promising targets for anticancer therapeutics. The traditional xenotransplantation assays used to investigate the properties of CSCs have technical and conceptual limitations (1). Recent studies have shown that leucine-rich repeat-containing G protein-coupled receptor 5 (*LGR5*) marks CSCs in human colorectal cancers (hCRCs) in vivo by lineage tracing of *LGR5-CreERT2* knockin hCRC organoids generated by CRISPR-Cas9–mediated gene editing (2, 3). Because most of the CSC markers are also expressed by normal stem cells (4–7), long-term CSC targeting may disrupt normal tissue homeostasis [e.g., liver injury after long-term LGR5-targeting (8)], whereas short-term CSC targeting leads to tumor regrowth (2, 9). Hence, identification of CSC-specific markers is essential. We previously showed that Dclk1, a differentiated tuft cell marker in normal intestine, marks tumor stem cells (TSCs) in mouse intestinal adenomas by lineage-tracing experiments (10). However, whether DCLK1 marks CSCs in hCRCs has not been elucidated by in vivo lineage tracing of the tumors. Furthermore, feasible strategies to target DCLK1$^+$ cells are necessary to realize a novel CSC-targeted therapy for hCRCs. Identification of a specific cell surface marker in Dclk1$^+$ cells can facilitate the sorting analysis of Dclk1$^+$ tumor cells and can also have the potential for future antibody therapeutics.

The IL-17 receptor family includes five members (IL17RA to IL17RE) (11). The heterodimer of IL17RA and IL17RC serves as a receptor for IL-17A and IL-17F to mediate Th17 immune response, and the heterodimer of IL17RA and IL17RB serves as a receptor for IL-25 to mediate Th2 immune response (12). Recent studies showed that the tuft cell is the main source of IL-25 in the intestine (13–15) and its receptor IL17RB is expressed by type 2 innate lymphoid cells (ILC2s) in the lamina propria (16). In case of helminth infection, induction of ILC2s by tuft cell-derived IL-25 results in IL-13 production and subsequent tuft cell and goblet cell hyperplasia for worm expulsion (13, 15). Although it has been indicated that IL17RB is also expressed in intestinal epithelial cells and plays an important role in intestinal inflammation (12, 17), its distinct role and expression pattern in intestinal tumorigenesis remain unknown.

In this study, we have elucidated that IL17RB is distinctively expressed in mouse Dclk1$^+$ intestinal tumor cells, and investigated the stem cell potential of *IL17RB*-expressing tuft cell-like cancer cells and the therapeutic effect of targeting them in hCRCs.

Results

IL17RB Marks Mouse Intestinal TSCs in an IL-13–Dependent Manner. To identify the cell surface marker distinctively expressed by Dclk1$^+$ tumor cells, we focused on IL17RB. Our microarray data showed that *Il17rb* mRNA expression is up-regulated in Dclk1$^+$ cells (18) and that Dclk1$^+$ tumor cells in the intestinal adenomas show similar mRNA and protein expression patterns to Dclk1$^+$ tuft cells in the normal intestine (18). Other investigators have also shown by microarray analysis of Trpm5$^+$ cells (19) and by single-cell RNA sequencing of small intestinal epithelial cells

Significance

Cancer stem cells, capable of self-renewing and giving rise to progeny cells in the tumor, have attracted attention as potential therapeutic targets. In this study, using genetically engineered mouse models, we showed that IL17RB, a tuft cell marker in the intestine, does not mark normal stem cells but marks tumor stem cells of mouse intestinal adenomas. Furthermore, using CRISPR-Cas9–mediated IL17RB-CreERT2 knockin human organoids, we showed that IL17RB marks human colorectal cancer stem cells by lineage tracing, and that long-term targeting of IL17RB$^+$ cells strongly suppressed the tumor growth in vivo. This study identifies IL17RB$^+$ cancer stem cells and preclinically validates them as a cancer therapeutic target.

Author contributions: N.G. and H.S. designed research; N.G., Y.Y., T.Y., T.M., and S.I. performed research; H. Maekawa, K.K., Y.S., H. Miyoshi, and M.M.T. contributed new reagents/analytic tools; N.G. and H.S. analyzed data; and N.G., A.F., T.C., and H.S. wrote the paper.

The authors declare no conflict of interest.

This article is a PNAS Direct Submission.

[1]To whom correspondence may be addressed. Email: seno@kuhp.kyoto-u.ac.jp.

This article contains supporting information online at www.pnas.org/lookup/suppl/doi:10.1073/pnas.1900251116/-/DCSupplemental.

Published online June 10, 2019.

(20) that *Il17rb* mRNA expression level is up-regulated in tuft cells. Until now, whether IL17RB is distinctively expressed on Dclk1$^+$ epithelial cells at the protein level remains unknown. Therefore, we performed flow cytometry analysis of EpCAM$^+$ intestinal epithelial cells from *Dclk1-EGFP* mice and identified that IL17RB is distinctively expressed at the protein level in Dclk1$^+$ tuft cells in the normal intestinal epithelium (Fig. 1*A*). Furthermore, flow cytometry analysis of EpCAM$^+$ intestinal tumor epithelial cells from *Dclk1-EGFP;Apc^{Min}* mice also showed distinctive IL17RB expression at the protein level in Dclk1$^+$ tumor cells, and qRT-PCR of sorted IL17RB$^+$Dclk1$^+$ cells confirmed significant up-regulation in mRNA expression of *Il17rb* and *Dclk1* (Fig. 1 *A* and *B*).

To further confirm the IL17RB expression pattern and to investigate the functional role of IL17RB in tumorigenesis, we generated *Il17rb-CreERT2-IRES-EGFP* knockin mice by inserting a *CreERT2-IRES-EGFP* cassette at the first ATG codon of the *Il17rb* allele (*SI Appendix*, Fig. S1). This enabled the visualization of IL17RB$^+$ cells and the deletion of IL17RB activity in these mice. Both heterozygous and homozygous mice were healthy and fertile and did not show any morphological abnormalities under normal conditions (*SI Appendix*, Fig. S2). We first confirmed EGFP expression under the IL17RB promoter in Dclk1$^+$ tuft cells. qRT-PCR of FACS-sorted GFP$^+$ cells from the EpCAM$^+$ intestinal epithelium of homozygous *Il17rb$^{CreERT2\text{-}IRES\text{-}EGFP/CreERT2\text{-}IRES\text{-}EGFP}$* mice showed significant up-regulation of *Dclk1, Pou2f3* [a transcriptional factor that is the master regulator of tuft cell differentiation (13)] and *Plcg2* [a tuft cell marker (19)] mRNA expression levels, and null expression of *Il17rb*, confirming the specific expression of GFP in Dclk1$^+$ tuft cells and the deletion of IL17RB activity (*SI Appendix*, Fig. S3 *A* and *B*). Immunostaining also demonstrated GFP$^+$ cells in the intestinal epithelium of *Il17rb$^{CreERT2\text{-}IRES\text{-}EGFP/CreERT2\text{-}IRES\text{-}EGFP}$* mice coexpressing tuft cell markers, such as Dclk1, POU2F3, and PLCG2, confirming that they are distinctively expressed in tuft cells (Fig. 1*C*). Next, we analyzed the intestinal tumors of *Il17rb$^{CreERT2/CreERT2}$;Apc^{Min}* mice. Although IL17RB has been reported to play an important role in some cancer cells (21, 22), the number of intestinal tumors did not differ in these mice (*SI Appendix*, Fig. S3 *C* and *D*), H&E staining did not reveal any morphological differences, and immunostaining revealed that the number of Dclk1$^+$ cells, Ki67$^+$ cells, and cleaved caspase 3$^+$ cells did not differ between the intestinal tumors of *Il17rb$^{CreERT2/CreERT2}$;Apc^{Min}* and *Apc^{Min}* mice (*SI Appendix*, Fig. S3 *E* and *F*). This suggests that for intestinal tumorigenesis in *Apc^{Min}* mice, *Il17rb* is functionally dispensable.

Next, to investigate the stem cell potential of *Il17rb*-expressing tumor cells, we performed lineage tracing in *Il17rb$^{CreERT2/CreERT2}$;Apc^{Min};Rosa26 tdTomato* mice (Fig. 1*D*). In the tumor epithelial cells, tdTomato expression was colocalized with Dclk1 after tamoxifen administration at day 1 and these tdTomato$^+$ cells expanded from the bottom to the top in these tumor cells at day 28, composing up to 23% of the entire tumors (Fig. 1 *E* and *F* and *SI Appendix*, Fig. S4 *C* and *D*). We confirmed by immunohistochemistry that these tdTomato$^+$ cells in the tumors included enteroendocrine cells, goblet cells, and Paneth cells (*SI Appendix*, Fig. S4*E*). These data show that *Il17rb*-expressing cells can self-renew and give rise to multiple lineages, confirming the stem cell potential of *Il17rb*$^+$ cells in the intestinal tumors without IL17RB activity. In the normal intestinal epithelium, we found that an extremely small number of the crypts (0.1%) showed tdTomato$^+$ clonal ribbons at day 28 in the normal small intestine as well as in the normal colon during homeostasis (Fig. 1*F* and *SI Appendix*, Fig. S4 *A* and *B*). These data suggest that stem cell potential of *Il17rb*-expressing cells was strictly limited in the normal small intestine as well as in the normal colon during homeostasis. It has been reported that IL17RB is also expressed by ILC2s in the lamina propria of the intestine (16). tdTomato$^+$ cells were also detectable both in the normal intestinal stroma and in the tumor stroma and colocalized with CD45 and c-KIT, but not with CD3, which is characteristic of ILC2s (Fig. 1 *E* and *F* and *SI Appendix*, Fig. S3*G*).

Because ILC2s are the predominant source of IL-13 in the intestine (23) and tuft cell differentiation in the normal intestine is tightly regulated by IL-13 (13–15), the presence of ILC2s in the tumor stroma prompted us to test whether differentiation of tuft cell-like tumor cells is also dependent on IL-13. To this end, we used an organoid culture system which allows for the analysis of isolated intestinal tumor epithelial cells in the absence of immune cells. Compared with that of in vivo tumors, the number of Dclk1$^+$ tuft cell-like tumor cells greatly decreased in the organoid cultures (*SI Appendix*, Fig. S5 *A* and *B*). We also performed lineage tracing in *Il17rb$^{CreERT2/CreERT2}$;Apc^{Min};Rosa26 tdTomato* tumor organoids. Interestingly, the tdTomato$^+$ cells were barely detectable and remained as single cells on day 4 after 4-hydroxytamoxifen (4-OHT) administration. However, in the organoids cultured with IL-13, tdTomato$^+$ cells increased in number and expanded in clusters (Fig. 1*G*), suggesting that the expansion of *Il17rb*-expressing tumor cells and their stem cell potential are dependent on IL-13. We also performed lineage tracing in *Dclk1$^{CreERT2/+}$;Apc^{Min};Rosa26 tdTomato* tumor organoids and the result was the same (*SI Appendix*, Fig. S5 *C* and *D*). Taken together, these data demonstrate that IL17RB marks mouse intestinal TSCs in an IL13-dependent manner.

IL17RB$^+$ Tuft Cell-Like Tumor Cells Comprise 2 Distinct Subsets. In the previous paper (10), we postulated that only Lgr5$^+$Dclk1$^+$ cells, but not Lgr5$^-$Dclk1$^+$ cells, mark TSCs in the intestinal tumors; however, because sorting of Dclk1$^+$ cells by antibody requires intracellular staining by fixation and permeabilization of the cells (10, 15), live cell analysis and transcriptome analysis of Lgr5$^+$ Dclk1$^+$ cells had not been feasible. IL17RB antibody enables sorting of live IL17RB$^+$ cells, and hence, the analysis of live Lgr5$^+$IL17RB$^+$ cells is now feasible to elucidate the TSC subset in IL17RB$^+$ cells in the intestinal tumors. To analyze the rare population of Lgr5$^+$IL17RB$^+$ tumor cells, we used *Lgr5^{CreERT2};Ctnnb1$^{lox(ex3)/lox(ex3)}$* mice, in which tumors are efficiently formed throughout the intestine after tamoxifen injection and histologically resemble those in *Apc* knockout mice (24). First, we sorted Lgr5$^-$IL17RB$^-$, Lgr5$^+$IL17RB$^-$, Lgr5$^-$IL17RB$^+$, and Lgr5$^+$ IL17RB$^+$ cells from the EpCAM$^+$ intestinal tumor epithelial cells of *Lgr5^{CreERT2}; Ctnnb1$^{lox(ex3)/lox(ex3)}$* mice 14 d after tamoxifen administration (Fig. 2*A*), and compared the organoid-forming capacity of each population. In comparison with Lgr5$^-$IL17RB$^-$ cells, organoid formation efficiency was significantly higher in Lgr5$^+$IL17RB$^-$ and Lgr5$^+$IL17RB$^+$ cells, but not in Lgr5$^-$IL17RB$^+$ cells (Fig. 2 *B* and *C*), confirming that Lgr5$^+$IL17RB$^+$ cells have TSC potential, whereas Lgr5$^-$IL17RB$^+$ cells have characteristics of differentiated cells.

Next, we evaluated the transcriptome of sorted Lgr5$^-$IL17RB$^-$, Lgr5$^+$IL17RB$^-$, Lgr5$^-$IL17RB$^+$, and Lgr5$^+$IL17RB$^+$ tumor cells by microarray analysis. The heat map showed up-regulation of tuft cell markers (e.g., *Il17rb*, *Dclk1*, *Pou2f3*, *Plcg2*) (20) in Lgr5$^-$IL17RB$^+$ cells, intestinal stem cell (ISC) markers (25) in Lgr5$^+$IL17RB$^-$ cells and both tuft cell and ISC markers in Lgr5$^+$IL17RB$^+$ cells (Fig. 2*D*). Gene set enrichment analysis (GSEA) also revealed enrichment of both tuft cell and ISC markers in Lgr5$^+$IL17RB$^+$ cells (Fig. 2*E*). GSEA comparing Lgr5$^+$IL17RB$^+$ cells and Lgr5$^-$IL17RB$^+$ cells revealed the enrichment of MYC-related genes (26), cyclin D1-related genes (27), and ISC signature genes in Lgr5$^+$IL17RB$^+$ cells, indicating the stem cell property of Lgr5$^+$IL17RB$^+$ cells (Fig. 2*F*). These results showed that IL17RB$^+$ tuft cell-like tumor cells in the intestinal tumors comprise two distinct subsets: highly differentiated tuft cell-like tumor cells (Lgr5$^-$IL17RB$^+$ cells) and tuft cell-like tumor cells with TSC potential (Lgr5$^+$IL17RB$^+$ cells). Once tumors are dissociated into single cells, Lgr5$^+$IL17RB$^+$ cells and Lgr5$^+$IL17RB$^-$ cells have almost the same clonogenicity (Fig. 2*B*),

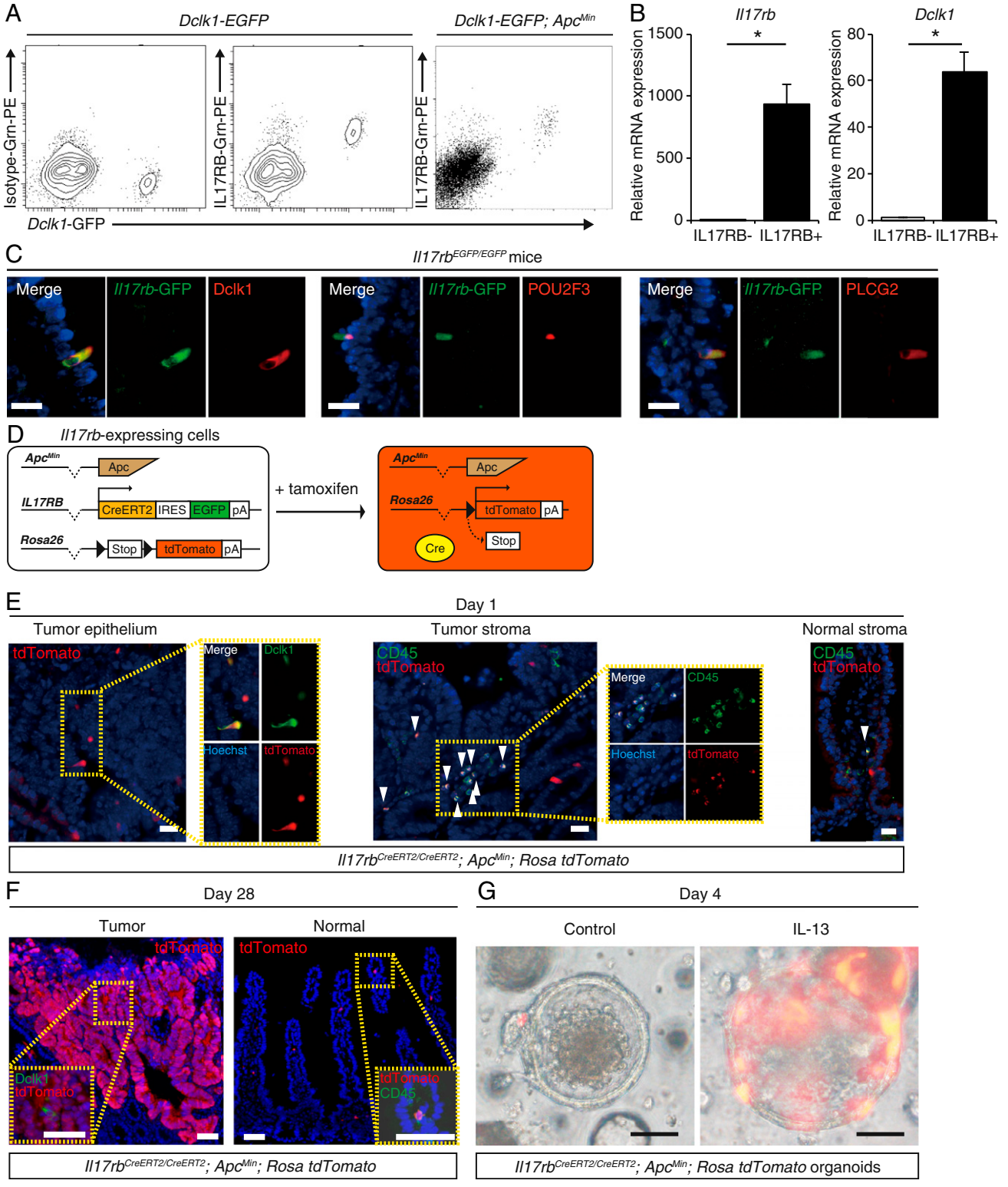

Fig. 1. IL17RB marks mouse intestinal TSCs in an IL13-dependent manner. (*A*) Flow cytometry of intestinal epithelial cells of *Dclk1-EGFP* mice and *Dclk1-EGFP;Apc^{Min}* mice stained with IL17RB antibody. (*B*) qRT-PCR of *Il17rb* and *Dclk1* expression in sorted Dclk1^{-}IL17RB^{-} and Dclk1^{+}IL17RB^{+} intestinal tumor epithelial cells. $n = 3$. $^{*}P < 0.05$; two-tailed unpaired Student's *t* test. Data are mean ± SEM. (*C*) GFP^{+} cells in *Il17rb$^{EGFP/EGFP}$* mice coexpressing tuft cell markers such as Dclk1, POU2F3, and PLCG2. (Scale bars, 20 μm.) (*D*) Strategy of lineage tracing of *Il17rb*-expressing cells in *Il17rb$^{CreERT2/CreERT2}$;Apc^{Min};Rosa26 tdTomato* mice. (*E*) At day 1 after tamoxifen administration, tdTomato expression was colocalized with Dclk1 in the tumor epithelial cells and tdTomato^{+}CD45^{+} cells (arrowheads) were detected both in the tumor stroma and in the normal intestinal stroma. (Scale bars, 20 μm.) (Magnification: *Left, Insets*, 1.2×; *Center, Insets*, 1.0×.) (*F*) At day 28 after tamoxifen administration, tdTomato^{+} cells expanded from the bottom to the top of the tumors, but in the normal intestine, tdTomato^{+} cells are hardly detectable in the epithelium and tdTomato^{+}CD45^{+} cells are detected in the stroma. (Scale bars, 50 μm.) (*G*) Images of tdTomato^{+} cells 4 d after 4-OHT administration in *Il17rb$^{CreERT2/CreERT2}$;Apc^{Min};Rosa26 tdTomato* tumor organoids cultured with or without IL-13. (Scale bars, 50 μm.)

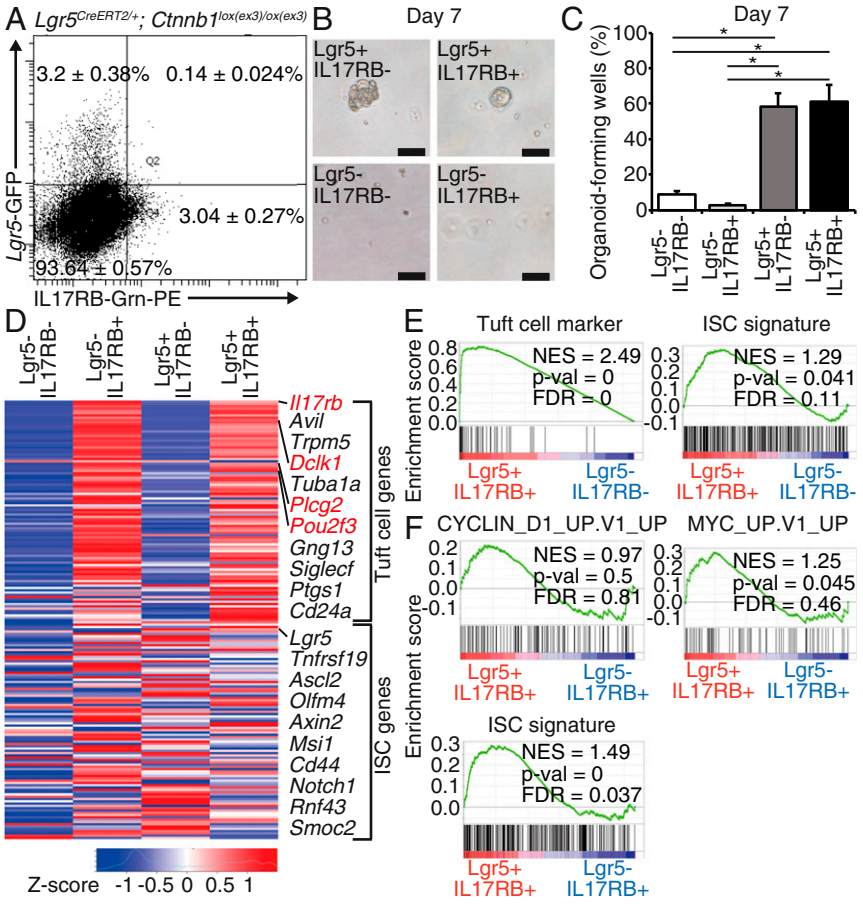

Fig. 2. IL17RB$^+$ tumor cells comprise two distinct subsets. (*A*) Tumor epithelial cells were sorted on the basis of IL17RB and Lgr5 expression in *Lgr5$^{CreERT2/+}$;Ctnnb1$^{lox(ex3)/ox(ex3)}$* mice 14 d after tamoxifen administration. The percentage of each cell population is presented as mean ± SEM of five independent experiments. (*B* and *C*) Representative images of organoids cultured from sorted Lgr5$^-$IL17RB$^-$, Lgr5$^+$IL17RB$^-$, Lgr5$^-$IL17RB$^+$, and Lgr5$^+$IL17RB$^+$ tumor cells (*B*) and the percentage of organoid-forming wells (*C*); 1000 cells of each population were cultured in each well. $n = 3$. (Scale bar, 100 μm.) *$P < 0.05$; two-tailed unpaired Student's t test. Data are mean ± SEM. (*D*) The heat map of microarray analysis of sorted Lgr5$^-$IL17RB$^-$, Lgr5$^+$IL17RB$^-$, Lgr5$^-$IL17RB$^+$, and Lgr5$^+$IL17RB$^+$ tumor cells. (*E* and *F*) GESA between Lgr5$^+$IL17RB$^+$ and Lgr5$^-$IL17RB$^-$ tumor cells (*E*) and between Lgr5$^+$IL17RB$^+$ and Lgr5$^-$IL17RB$^+$ tumor cells (*F*). FDR, false-discovery rate; NES, normalized enrichment score.

and the proportion of Lgr5$^+$IL17RB$^+$ cells is much lower than that of Lgr5$^+$IL17RB$^-$ cells (Fig. 2*A*). However, IL17RB$^+$ cells give rise to about 23% of the in vivo tumors at day 28 (*SI Appendix*, Fig. S4*D*), which is comparable to the percentage (up to 30%) of the progeny of Lgr5$^+$ cells at day 24 in the traced tumors (28). Provided that Lgr5$^-$IL17RB$^+$ cells are highly differentiated cells (Fig. 2*C*), Lgr5$^+$IL17RB$^+$ cells may be the subset of Lgr5$^+$ tumor cells, which mainly give rise to progeny cells in the in vivo tumors. Organoid-forming capacity may somewhat differ from the stem cell potential of each cell population in the tumors in situ, because tumor cells rely on cell-to-cell interactions and signals from the microenvironment (1, 2). These issues have been previously raised regarding the transplantation experiments of cancer stem cells (1). Importantly, GSEA comparing Lgr5$^+$IL17RB$^+$ cells and Lgr5$^+$IL17RB$^-$ cells revealed the enrichment of KRAS signaling and NF-κB signaling in Lgr5$^+$IL17RB$^+$ cells (*SI Appendix*, Fig. S6). This signaling is essential for the acquisition of stem cell-like properties in the tumor initiation (29, 30) and also for a drift toward the clonal expansion in the intestinal stem cells (31), suggesting the predominant potential of stem cell-like property in Lgr5$^+$IL17RB$^+$ cells over Lgr5$^+$IL17RB$^-$ cells in vivo. Because abrogating entire Lgr5$^+$ cells entails liver injury (8), targeting Lgr5$^+$IL17RB$^+$ cells may be the rational therapeutic strategy to avoid disruption of normal tissue homeostasis.

IL17RB Marks Tuft Cell-Like hCRC Stem Cells Independently of IL-13. Next, we set out to investigate whether IL17RB marks hCRC stem cells by lineage tracing. Immunostaining for tuft cell marker PLCG2 in normal human colonic epithelium and CRCs stably marked distinct slender tuft cells and tuft cell-like cancer cells, respectively (*SI Appendix*, Fig. S7*A*); we used it for screening hCRCs that have a subpopulation of tuft cell-like cancer cells. Recently, we established hCRC organoid/spheroid lines and patient-derived tumor xenografts by an improved method (32, 33). We examined 57 cases of hCRCs in which organoids or patient-derived tumor xenografts were successfully established. In the primary tumors, a distinct population (0.08–1.9%) of tuft cell-like cancer cells was detected in 10 cases (18%, tuft cell-like prominent) but was not detected in the remaining 47 cases (82%, tuft cell-like nonprominent) (*SI Appendix*, Fig. S7 *B–D*). This indicates that while the tuft cell-like differentiation capacity may be disrupted in more than half of the hCRCs, there is a distinct subtype of hCRCs with conserved tuft cell-like differentiation properties, as previously reported (10, 34).

For further experiments, we focused on two cases (case Z and case H) that showed PLCG2$^+$ tuft cell-like cancer cells both in the primary tumors and in the xenograft transplantation tumors (Fig. 3*A*). To perform lineage tracing of IL17RB$^+$ cancer cells in hCRCs, we inserted a 2A-CreERT2 cassette in the endogenous *IL17RB* gene locus immediately at the 5′ end of the endogenous stop codon by CRISPR-Cas9–mediated gene editing in the hCRC organoids (Fig. 3*B* and *SI Appendix*, Fig. S8 *A–C*). The resulting IL17RB-2A-CreERT2 fusion protein is automatically cleaved into functional IL17RB and CreERT2 protein, thereby maintaining endogenous IL17RB function (*SI Appendix*, Fig. S8*D*). This construct is different from the *Il17rb-CreERT2* mice in which CreERT2 is inserted at the first ATG, resulting in deletion of *Il17rb* in homozygous mice (*SI Appendix*, Figs. S1 and S3*B*). We thereafter introduced a CMV-LoxP-DsRed-LoxP-eGFP reporter by lentivirus transduction. These organoids constitutively express DsRed and upon tamoxifen administration, the fluorescent protein expression irreversibly switches from DsRed to GFP in *IL17RB*-expressing cells, enabling the lineage tracing of these cells (Fig. 3*C*). We finally generated three

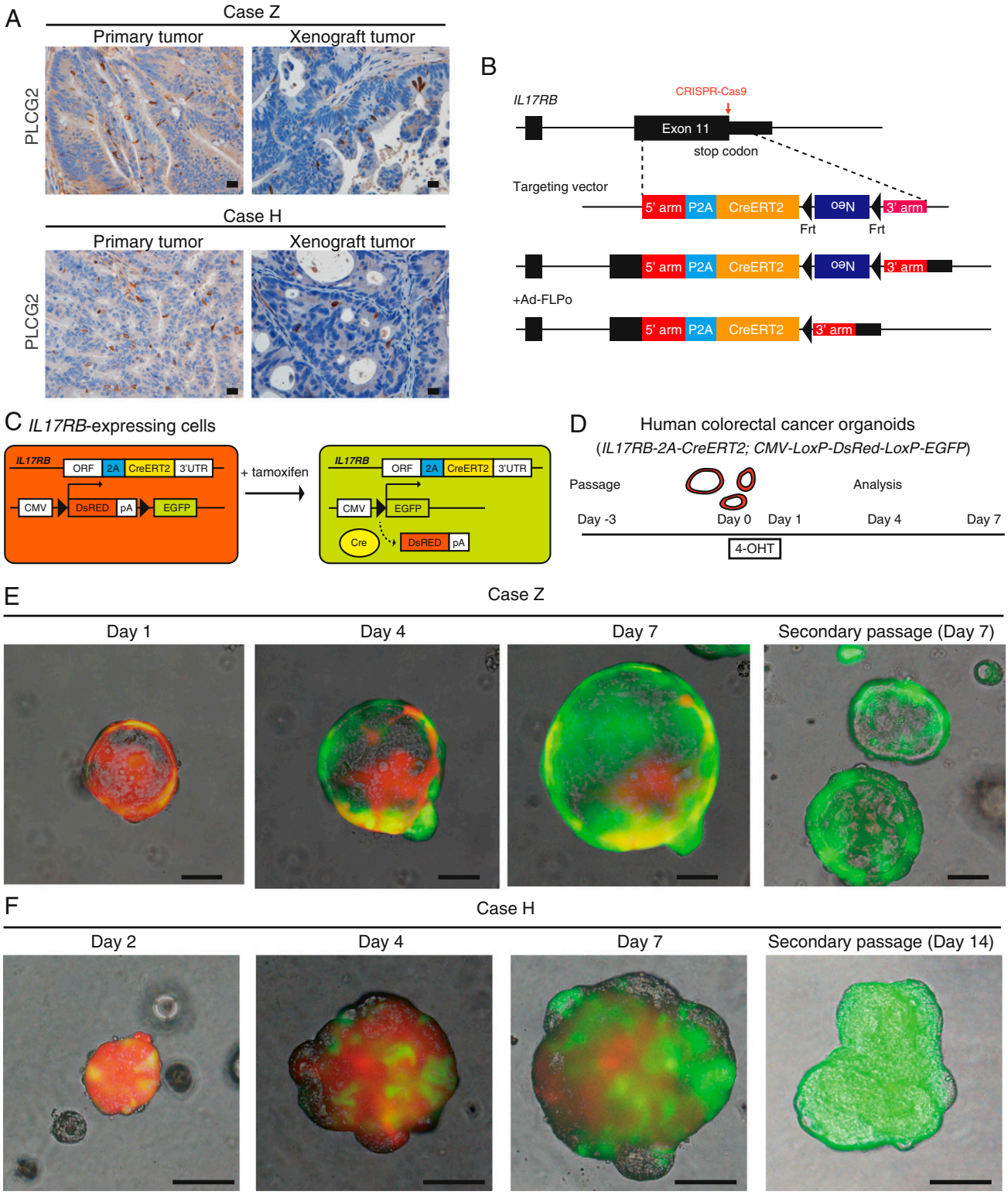

Fig. 3. IL17RB marks hCRC stem cells independently of IL-13. (*A*) Immunostaining of PLCG2 revealed that tuft cell-like differentiation was recapitulated in the xenograft tumors established from tuft cell-like prominent hCRCs. (Scale bars, 20 μm.) (*B*) Strategy to insert 2A-CreERT2 cassette into the endogenous *IL17RB* gene locus immediately at 5′ end of the endogenous stop codon by CRISPR-Cas9–mediated gene editing in hCRC organoids. (*C* and *D*) Strategy of lineage tracing in *IL17RB-2A-CreERT2; CMV-LoxP-DsRed-LoxP-eGFP* hCRC organoids. These organoids constitutively express DsRed and upon tamoxifen administration, the fluorescent protein expression irreversibly switches from DsRed to GFP in *IL17RB*-expressing cells. (*E*) Time-course images of *IL17RB-2A-CreERT2 (homozygous);CMV-LoxP-DsRed-LoxP-eGFP* hCRC organoids of case Z after 4-OHT administration. (Scale bars, 100 μm.) (*F*) Time-course images of *IL17RB-2A-CreERT2 (heterozygous);CMV-LoxP-DsRed-LoxP-eGFP* hCRC organoids of case H after 4-OHT administration. (Scale bars, 100 μm.)

clonal *IL17RB-2A-CreERT2;CMV-LoxP-DsRed-LoxP-eGFP* hCRC organoids (homozygous and heterozygous knockin organoids of case Z and heterozygous knockin organoids of case H). We first performed lineage tracing of homozygous knockin hCRC organoids of case Z (Fig. 3*D*). Twenty-four hours after 4-OHT administration, *IL17RB*-expressing GFP$^+$ cells appeared in a small subset of DsRed$^+$ cells and these GFP$^+$ cells rapidly expanded, replacing most of the DsRed$^+$ cells by day 7 (Fig. 3*E*). These GFP$^+$ cells also gave rise to secondary organoids after passage, indicating that the *IL17RB*-expressing hCRC cells are capable of self-renewal and giving rise to progeny cells. To exclude the possibility that different fluorescent protein expressions affect the cell growth in the organoids, we continuously administered 4-OHT to the engineered organoids with several passages until the GFP$^+$ cells completely overtook the organoids (GFP$^+$ organoids), and compared the organoid growth rate with the organoids without 4-OHT administration (DsRed$^+$ organoids) (*SI Appendix*, Fig. S9 *A*–*C*). The organoid growth rate between GFP$^+$ organoids and DsRed$^+$ organoids was the same (*SI Appendix*, Fig. S9 *D* and *E*).

To directly visualize how the *IL17RB*-expressing CSCs self-renew and give rise to progeny cells, we performed time-lapse imaging of *IL17RB-2A-CreERT2; CMV-LoxP-DsRed-LoxP-eGFP* hCRC organoids after 4-OHT administration using two-photon excitation incubator microscopy, which allows long-term high-resolution imaging with minimal photobleaching and phototoxicity. The movie shows the time course of GFP$^+$ cells proliferating and replacing the existing DsRed$^+$ cells in the organoids (Movie S1). We also confirmed that *IL17RB*-expressing cells reproducibly mark CSCs in other engineered *IL17RB-2A-CreERT2;CMV-LoxP-DsRed-LoxP-eGFP* hCRC organoids (heterozygous knockin in case Z and heterozygous knockin in case H) (Fig. 3*F* and *SI Appendix*, Fig. S8*E*). In case H, the expansion of GFP$^+$ cells is relatively slow compared with that in case Z, suggesting that the characteristics of IL17RB$^+$ CSCs differ between each hCRC.

Surprisingly, unlike the result of lineage tracing in mouse intestinal adenomas, IL17RB marks CSCs in these hCRC organoids without the addition of IL-13 in the culture medium and the same result was observed even after withdrawal of serum. We sought to investigate the factors that render IL-13 dispensable for the maintenance of IL17RB$^+$ CSCs and their stem cell property in tuft cell-like prominent hCRCs. To this end, we compared the mRNA expression levels of *IL4R* (the receptor for IL-13), *STAT6* [the essential mediator of IL-13/IL-4R signaling (14, 35)] and *POU2F3* [tuft cell lineage regulator (13)] between the cancer organoids and the normal organoids generated from the adjacent normal colorectal mucosa of case Z and case H, which allows the identification of deregulated signals that might occur during tuft cell-like differentiation in the absence of immune cells. Interestingly, we observed that IL-13/IL-4R signaling pathways were down-regulated and *POU2F3* expression was up-regulated in the cancer organoids of both case Z and case H (Fig. 4*A*). Recently, a tuft cell-like variant of small-cell lung cancer with high *POU2F3* expression was reported (36), and our results also imply variant hCRCs with high *POU2F3* expression and autonomous tuft cell-like differentiation properties. Immunohistochemistry confirmed that POU2F3 was specifically expressed in PLCG2$^+$ tuft cell-like cancer cells in the primary tumors (Fig. 4*B*). POU2F3$^+$ cells were also stably detected in the organoids of tuft cell-like prominent hCRCs that were not treated with IL-13 (Fig. 4*B*), whereas in the organoids of human normal colonic epithelia, mouse small intestinal adenomas, and mouse colonic adenomas, POU2F3$^+$ cells were stably detected only after IL-13 administration (Fig. 4 *D*, *F*, and *H*). Furthermore, in the organoids of tuft cell-like prominent hCRCs, *POU2F3* mRNA expression level was not up-regulated after IL-13 administration (Fig. 4*C*), whereas in the organoids of human normal colonic epithelia, mouse small intestinal adenomas, and mouse colonic adenomas, *POU2F3* mRNA expression levels were significantly up-regulated after IL-13 administration (Fig. 4 *E*, *G*, and *I*). These data suggest the cancer epithelial cell-autonomous *POU2F3* expression and disrupted response to IL-13 in tuft cell-like prominent hCRCs.

To further investigate hCRCs with autonomous *POU2F3* expression, we analyzed The Cancer Genome Atlas (TCGA)

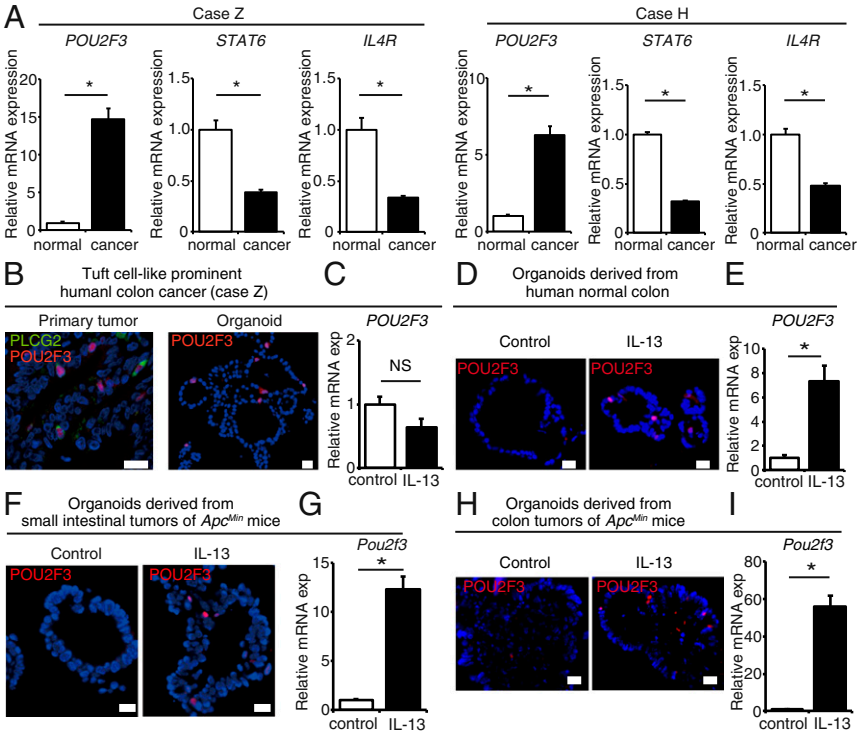

Fig. 4. Autonomous up-regulation of POU2F3 and tuft cell-like cancer cell differentiation in tuft cell-like prominent hCRCs. (*A*) qRT-PCR of *POU2F3*, *STAT6*, and *IL4*R mRNA expression between tuft cell-prominent hCRC organoids and normal organoids generated from the adjacent normal colorectal mucosa of case Z and case H. $n = 3$. (*B*) Colocalization of POU2F3 and PLCG2 in the primary tumor of case Z. POU2F3$^+$ cells were stably detected in the organoids of case Z without IL-13 administration. (*C*) *POU2F3* mRNA expression level was not up-regulated after IL-13 administration in the organoids of tuft cell-like prominent hCRCs. $n = 3$. (*D*–*I*) POU2F3$^+$ cells were stably detected only after IL-13 administration in the organoids of human normal colonic epithelia (*D*), mouse small intestinal adenomas (*F*), and mouse colonic adenomas (*H*). *POU2F3* mRNA expression levels were significantly up-regulated after IL-13 administration in the organoids of human normal colonic epithelia (*E*), mouse small intestinal adenomas (*G*), and mouse colonic adenomas (*I*). *$P < 0.05$; NS, not significant; two-tailed unpaired Student's *t* test. Data are mean ± SEM. (Scale bars, 20 μm.)

transcriptome data of colon and rectal cancers. *POU2F3* mRNA expression in both colon and rectal cancers correlated with the expression of tuft cell markers, such as *AVIL*, *GNG13*, *SH2D6*, and *TRPM5* (*SI Appendix*, Fig. S10*A*), but did not correlate with *IL4R* or *STAT6* expression (*SI Appendix*, Fig. S10*B*). These results further suggest the autonomous expression of *POU2F3* and tuft cell-like differentiation in a subset of hCRCs, which probably leads to the maintenance of IL17RB$^+$ CSCs and their stem cell property, independent of IL-13. We also tested whether IL17RB-mediated signaling plays an essential role in the autonomous *POU2F3* expression in these hCRCs. Because tuft cells produce IL-25 (13, 15), there are possibilities that IL17RB signaling is triggered by autocrine secretion of IL-25. We administered IL-25 or anti–IL-25 neutralizing antibody to the hCRC organoids (*SI Appendix*, Fig. S11*A*); however, *POU2F3* expression levels were not affected (*SI Appendix*, Fig. S11*C*) and the lineage-tracing experiments of *IL17RB*-expressing cells showed no difference compared with those of the control organoids (*SI Appendix*, Fig. S11*B*). We also knocked down *IL17RB* in the hCRC organoids; the expression levels of tuft cell markers such as *POU2F3* and *PLCG2* were not affected (*SI Appendix*, Fig. S11*D*), and the organoid-forming capacity was not affected either (*SI Appendix*, Fig. S11 *E* and *F*). These experiments showed that in hCRCs, the function of IL17RB itself does not play an essential role in the cell-autonomous expression and self-renewal of IL17RB$^+$ tuft cell-like cancer stem cells.

Next, we transplanted these *IL17RB-2A-CreERT2;CMV-LoxP-DsRed-LoxP-eGFP* hCRC organoids subcutaneously in immune-deficient mice and administered tamoxifen 2 mo posttransplantation (Fig. 5*A*). In case Z, *IL17RB*-expressing GFP$^+$ cells initially coexpressed POU2F3$^+$ and PLCG2$^+$ tuft cell-like cancer cells (Fig. 5*B*), and by day 16 these GFP$^+$ cells rapidly expanded, replacing most of the DsRed$^+$ cells in the tumors (Fig. 5 *C* and *D*). We transplanted these tamoxifen-treated xenograft tumors into secondary recipient immune-deficient mice; GFP$^+$ cells gave rise to the secondary tumors, suggesting the long-term self-renewal capacity of the IL17RB$^+$ cells (*SI Appendix*, Fig. S8*F*). We confirmed these results both in nude mice (*SI Appendix*, Fig. S8*G*)

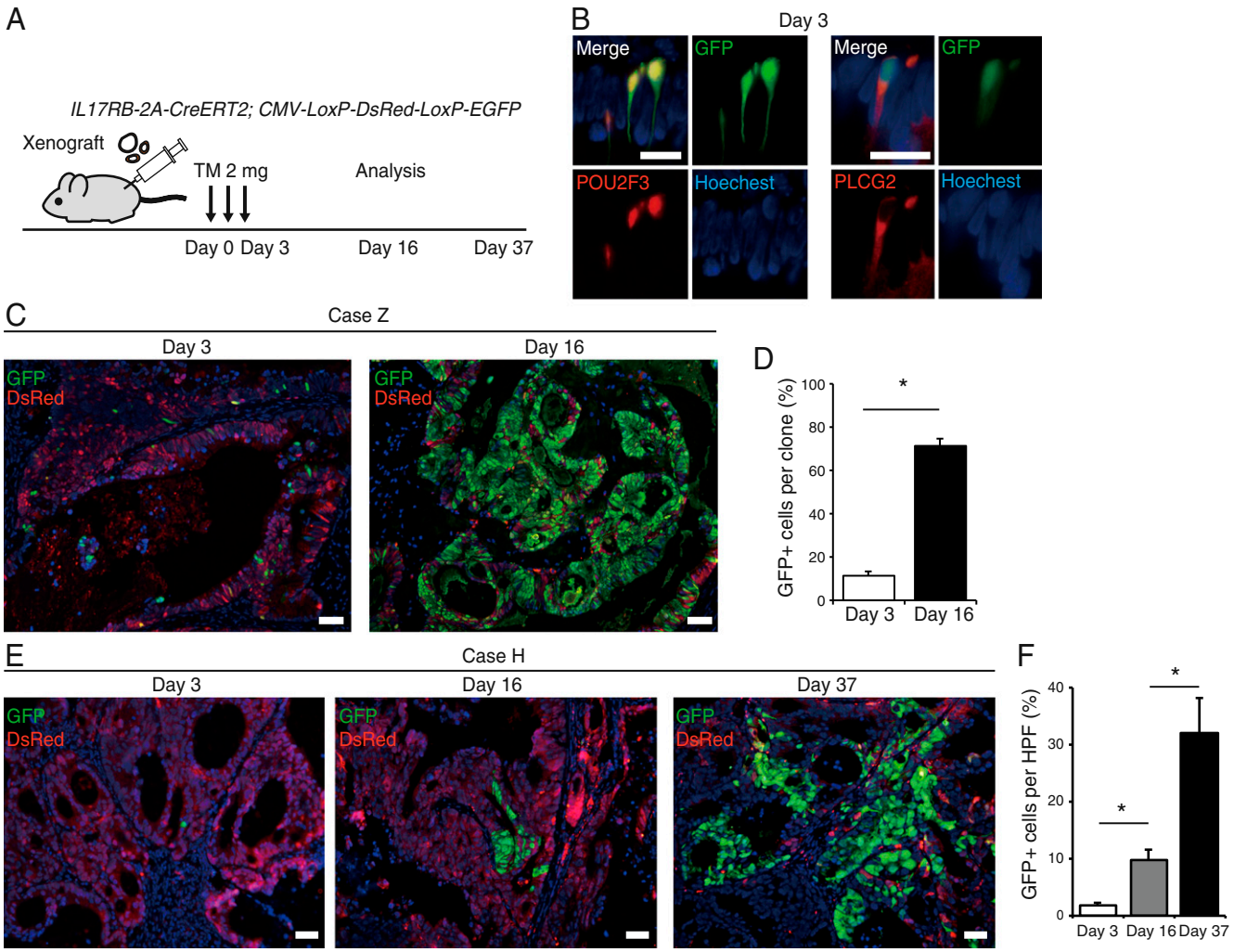

Fig. 5. IL17RB marks hCRC stem cells in vivo. (*A*) Strategy of lineage tracing in xenograft tumors of *IL17RB-2A-CreERT2;CMV-LoxP-DsRed-LoxP-eGFP* hCRC organoids. (*B*) Colocalization of POU2F3 with GFP reporter and PLCG2 with GFP reporter, respectively. (Scale bars, 20 μm.) (*C* and *D*) Lineage tracing of xenograft tumors of *IL17RB-2A-CreERT2 (homozygous);CMV-LoxP-DsRed-LoxP-eGFP* hCRC organoids of case Z transplanted in NOD/SCID mice subcutaneously. Images of GFP reporter at day 3 gave rise to progeny cells and spread to most parts of the clones by day 16 after tamoxifen injection (*C*). Quantification of the percentage of GFP$^+$ cells per clone at day 3 and at day 16. $n = 20$ (*D*). (*E* and *F*) Lineage tracing of xenograft tumors of *IL17RB-2A-CreERT2;CMV-LoxP-DsRed-LoxP-eGFP* hCRC organoids of case H transplanted in NOD/SCID mice subcutaneously. Images of GFP reporter at day 3 slowly gave rise to progeny cells and spread to the tumors by day 37 after tamoxifen injection (*E*). Quantification of the percentage of GFP$^+$ cells in HPF wherein GFP$^+$ cells were present at days 3, 16, and 37. $n = 10$ (*F*). *$P < 0.05$; two-tailed unpaired Student's *t* test. Data are mean ± SEM. (Scale bars, 50 μm.)

and NOD/SCID mice (Fig. 5*C*), suggesting again that IL17RB$^+$ cancer cells and their stem cell potential in tuft cell-like prominent hCRCs are maintained regardless of tumor microenvironment. We also observed the same results in in vivo lineage tracing of case H, although the expansion of GFP$^+$ cells was relatively slow (Fig. 5 *E* and *F*), as observed in lineage tracing of the organoids. These results confirmed that IL17RB marks CSCs in tuft cell-like prominent hCRCs.

Long-Term Ablation of IL17RB$^+$ CSCs Strongly Suppressed Tumor Growth. Finally, to test the therapeutic effect of targeting IL17RB$^+$ CSCs in hCRC, we introduced a CMV-LoxP-DsRed-LoxP-iCaspase9-2A-eGFP reporter to *IL17RB-2A-CreERT2* hCRC organoids by lentivirus transduction. Upon tamoxifen administration, the fluorescent protein expression in *IL17RB*-expressing cells switches from DsRed to GFP with iCapspase9 expression; therefore, concomitant administration of 4-OHT and dimerizer can induce the apoptosis of *IL17RB*-expressing GFP$^+$ CSCs (Fig. 6*A*). Whereas *IL17RB*-expressing GFP$^+$ cells appeared in a small subset of the organoids and gave rise to progeny cells after 4-OHT administration, *IL17RB*-expressing GFP$^+$ cells were depleted in the organoids after concomitant 4-OHT and dimerizer administration, showing the successful ablation of *IL17RB*-expressing cells (Fig. 6*B*). Furthermore, the organoid growth was strongly suppressed by the continuous ablation of IL17RB$^+$ CSCs (Fig. 6 *B* and *C*). After 6 d of L17RB$^+$ cell ablation, POU2F3$^+$ cells were not detected by immunohistochemistry (Fig. 6*D*) and additional 4-OHT administration to the organoids does not produce GFP$^+$ cells (*SI Appendix*, Fig. S12 *A* and *B*), confirming again the depletion of tuft cell-like cancer cells. However, 2 d after cessation of the dimerizer administration, reappearance of POU2F3$^+$ tuft cell-like cancer cells was observed in the organoids (Fig. 6*D*). In these organoids, regrowth was observed (Fig. 6 *E* and *F*) and readministration of 4-OHT resulted in the appearance of GFP$^+$ cells that proliferate and overtake the organoids (Fig. 6 *E* and *F*), showing that newly generated IL17RB$^+$ cells also possesses stem cell potentials. Readministration of 4-OHT and dimerizer depleted GFP$^+$ cells and attenuated the organoid growth again (Fig. 6 *E* and *F*), indicating the importance of continuous targeting of IL17RB$^+$ cells.

We next validated the effect of IL17RB$^+$ CSC targeting in vivo. Injection of tamoxifen and dimerizer for 6 d to the immunodeficient mice with the xenograft tumors of the engineered organoids resulted in the depletion of PLCG2$^+$ POU2F3$^+$ tuft cell-like cancer cells and tumor stasis (Fig. 7 *A* and *B* and *SI Appendix*, Fig. S12 *C* and *D*). However, discontinuation of ablation resulted in the reappearance of PLCG2$^+$ POU2F3$^+$ tuft cell-like cancer cells and tumor regrowth (Fig. 7 *A* and *B* and *SI Appendix*, Fig. S12 *C* and *D*). These results imply that the tumor regrowth is fueled by IL17RB$^+$ cells, which constantly reappear even after depletion of IL17RB$^+$ cells. To overcome this, we next validated the effect of long-term continuous IL17RB$^+$ CSC targeting in vivo. Continuous injection of tamoxifen and dimerizer for 28 d resulted in strong tumor growth suppression and complete regression of one of the six tumors in vivo (Fig. 7 *C* and *D* and *SI Appendix*, Fig. S12*E*). Furthermore, histological analyses of the remaining five tumors revealed a dramatic collapse of their glandular architecture and cellular structure (Fig. 7*E*). Immunohistochemistry revealed depletion of PLCG2$^+$ POU2F3$^+$ tuft cell-like cancer cells and the decreased number of Ki67$^+$ cells in these tumors (Fig. 7*F*). These data suggest the significant effect of long-term IL17RB$^+$ cell targeting. Finally, we orthotopically transplanted the engineered organoids to the rectum of immunodeficient mice and administered tamoxifen and dimerizer; IL17RB$^+$ cell ablation significantly reduced the tumor engraftment rate (*SI Appendix*, Fig. S13), suggesting the

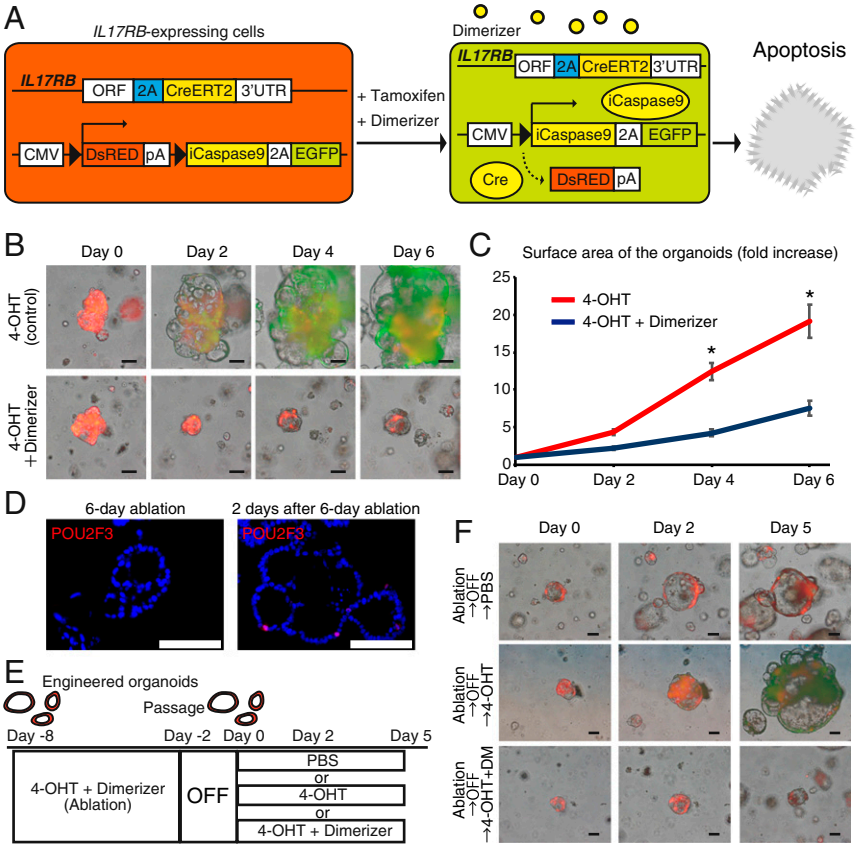

Fig. 6. Ablation of IL17RB$^+$ CSCs attenuates the organoid growth. (*A*) Strategy of ablation of *IL17RB*-expressing cells in the organoids. (*B*) Time-course images of *IL17RB-2A-CreERT2 (homozygous);CMV-LoxP-iCaspase9-2A-eGFP* hCRC organoids of case Z after 4-OHT or concomitant 4-OHT and dimerizer administration. (Scale bars, 100 μm.) (*C*) The organoid growth was strongly suppressed by the continuous ablation of IL17RB$^+$ CSCs. $n = 20$. *$P < 0.05$; two-tailed unpaired Student's t test. Data are mean ± SEM. (*D*) After 6 d of L17RB$^+$ cell ablation in the organoids, POU2F3$^+$ tuft cell-like cancer cells were not detected by immunohistochemistry; however, 2 d after cessation of the dimerizer administration, reappearance of POU2F3$^+$ tuft cell-like cancer cells was observed. (Scale bars, 100 μm.) (*E* and *F*) IL17RB$^+$ cells in the organoids were ablated for 6 d and the ablation was discontinued for 2 d. In these organoids, regrowth was observed and readministration of 4-OHT resulted in the appearance of GFP$^+$ cells that proliferate and overtake the organoids. Additional continuous administration of 4-OHT and dimerizer-depleted GFP$^+$ cells and attenuated the organoid growth. (Scale bars, 100 μm.)

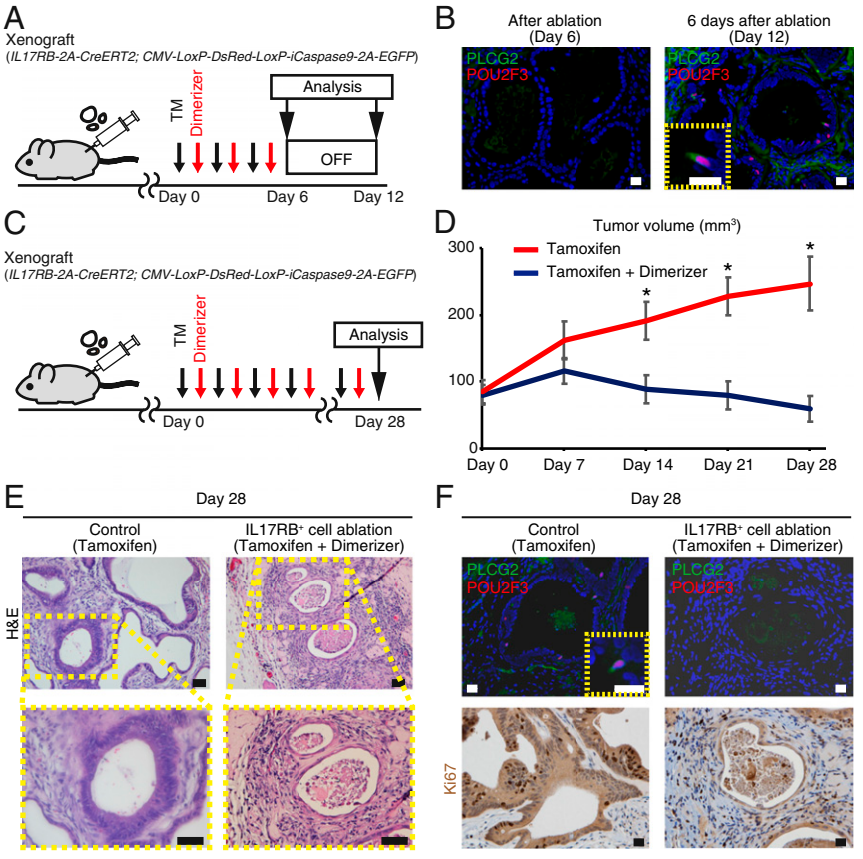

Fig. 7. Long-term ablation of IL17RB$^+$ CSCs strongly suppressed tumor growth in vivo. (*A*) Strategy to validate depletion of tuft cell-like cancer cells after Il17RB$^+$ cell ablation and reappearance of tuft cell-like cancer cells after the cessation of the ablation in vivo. Dimerizer and tamoxifen were administered alternately every other days for 6 d and thereafter the treatment was discontinued. (*B*) Immunostaining revealed depletion of PLCG2$^+$ POU2F3$^+$ tuft cell-like cancer cells after ablation; however, PLCG2$^+$ POU2F3$^+$ tuft cell-like cancer cells reappeared 6 d after discontinuation of the ablation. (Scale bars, 20 μm.) (*C*) Strategy of long-term ablation of *IL17RB*-expressing cells in vivo. Dimerizer and tamoxifen were administered alternately every other days for 28 d. (*D*) Continuous ablation of *IL17RB*-expressing cells in the xenograft tumors of case Z resulted in strong tumor growth suppression. $n = 6$. $^*P < 0.05$; two-tailed unpaired Student's t test. Data are mean ± SEM. (*E* and *F*) H&E staining (*E*) and immunostaining for PLCG2, POU2F3, and Ki67 (*F*) in the tumors after 28 d of IL17RB$^+$ cell ablation. (Scale bars, 50 μm in *E*; 20 μm in *F*.)

therapeutic effect of targeting IL17RB$^+$ cells in the primary tumors with the microenvironment. Taken together, these results demonstrate that long-term IL17RB$^+$ cell targeting may be a novel therapeutic strategy for tuft cell-like prominent hCRCs.

Discussion

In this study, we elucidate that IL17RB, a tuft cell marker, marks TSCs of mouse intestinal adenomas and CSCs of hCRCs by distinct mechanisms (*SI Appendix*, Fig. S14) and validate the therapeutic effect of targeting IL17RB$^+$ CSCs. While previous reports show IL-25 expression by tuft cells in the intestinal epithelium (13–15) and IL17RB (the receptor for IL-25) expression by ILC2s (16, 23), we noticed IL17RB expression by tuft cells. Although the previous transcriptome analysis showed up-regulated *Il17rb* mRNA expression in tuft cells (18–20), our work shows that IL17RB is distinctively expressed in Dclk1$^+$ intestinal epithelial cells at the protein level and that IL17RB marks mouse intestinal TSCs. Identification of IL17RB enables further analysis of two distinct subsets of tuft cell-like tumor cells: highly differentiated tuft cell-like tumor cells (Lgr5$^-$IL17RB$^+$ cells) and tuft cell-like tumor cells with TCS potential (Lgr5$^+$IL17RB$^+$ cells). Furthermore, we found that Lgr5$^+$IL17RB$^+$ tumor cells are the subset of Lgr5$^+$ tumor cells with up-regulated KRAS signaling and NF-κB signaling, which is essential for the acquisition of stem cell property in the tumor initiation (29–31). Identification of markers specifically expressed by Lgr5$^+$IL17RB$^+$ tumor cells will help to elucidate the further mechanisms in the future.

The combination of CRISPR-Cas9 technology and organoid culture (37) enabled the lineage-tracing experiments in human cancers. LGR5 has been the only marker tested to mark human CSCs by lineage tracing (2, 3). However, long-term LGR5 targeting causes liver toxicity (8). Tuft cell-like cancer cells were detected in a subset of hCRCs. Our work shows that IL17RB marks tuft cell-like CSCs in these hCRCs by lineage-tracing experiments and that long-term targeting of IL17RB$^+$ CSCs strongly suppressed tumor growth in vivo. Because IL17RB is not expressed by normal stem cells in mouse models and a complete absence of tuft cells does not affect global immunity or intestinal epithelium formation in *Pou2f3*-deficient mice (13), IL17RB$^+$ cells may be amenable for long-term targeting. Furthermore, because tuft cell-like cancer cells in hCRCs have similar protein-expression patterns to tuft cells and are stably detectable by immunostaining for PLCG2 or other tuft cell markers, such as hematopoietic prostaglandin-D synthases (34), we could readily identify hCRCs with a subpopulation of IL17RB$^+$ tuft cell-like cancer cells from biopsy samples, which facilitate the selection of candidate patients for future therapy.

IL17RB has been reported to play an important role in some cancers (21, 38, 39). For example, IL17RB–IL17B signaling has been reported to play an essential role in breast cancer tumorigenesis (38) and pancreatic cancer metastasis (21). IL-17B antagonizes IL-25-mediated mucosal inflammation in the mouse colon (17). Our data revealed that the deletion of IL17RB activity did not affect the intestinal tumorigenesis in Apc^{Min} mice and knockdown of *IL17RB* did not affect hCRC organoid growth, indicating the organ context-dependent role of IL17RB in the tumors. From these results, it should be possible to target IL17RB$^+$ CSCs for antibody therapeutics by employing antibody–drug conjugates, similar to previous reports that show targeting of LGR5$^+$ cells (40), rather than blocking the receptor signal.

The expansion of IL17RB$^+$ tuft cell-like tumor cells in mouse intestinal adenomas is tightly regulated by IL-13. ILC2s are the predominant source of IL-13 in the intestine (23); however, other immune cells, such as Th2 cells (41), NK cells (42), and mast cells (43) also produce IL-13 in the intestine. Although we have shown the existence of ILC2s in the tumor stroma, the essential sources of IL-13 in the tumor microenvironment still

remain controversial and will be further evaluated in a future study. Because the tumor transition from adenoma to carcinoma entails higher grades of dysplasia with lower differentiation capacities (44), it is plausible that tuft cell-like cancer cells were not detectable in over half of hCRCs. However, we found a subset of hCRCs with tuft cell-like cancer cells, namely the tuft cell-like prominent hCRCs. In these hCRCs, tuft cell-like cancer cells have similar protein (e.g., PLCG2, POU2F3, and IL17RB) expression patterns to tuft cells; however, tuft cell-like differentiation was cancer cell-autonomous, rendering IL-13 dispensable for the maintenance of IL17RB$^+$ CSCs (*SI Appendix*, Fig. S14). Up-regulation of *POU2F3*, a master regulator of tuft cell differentiation (13), could be the cause of the distinct phenotype observed in tuft cell-like prominent hCRCs. The IL-13/IL-4R signaling pathway was down-regulated in tuft cell-like prominent hCRCs. The expression of *POU2F3* in tuft cell-like prominent hCRCs is cancer epithelial cell-autonomous and regulated by a different mechanism from that of mouse intestinal adenomas or human normal colonic epithelium, which is dependent on the IL-13/IL-4R signaling pathway. Our results also show that the function of IL17RB does not play an important role in the cell-autonomous expression and self-renewal of tuft cell-like CSCs. Although ChIP-seq analysis of POU2F3 in small-cell lung cancer with high *POU2F3* expression revealed that it activates a set of enhancers to promote the expression of tuft cell lineage genes (36), factors up-regulating *POU2F3* expression in these variant cancers remain unknown. Similarly, we could not identify any specific gene mutations or putative copy-number alterations of *POU2F3* in hCRCs expressing high *POU2F3* levels in TCGA data; further accumulation of tuft cell-like prominent hCRCs is necessary to elucidate the intrinsic factors up-regulating *POU2F3* expression.

In conclusion, we elucidated that IL17RB marks TSCs of mouse intestinal adenomas and tuft cell-like CSCs in a subset of hCRCs. Ablation experiments of IL17RB$^+$ CSCs in vivo preclinically validated IL17RB$^+$ CSCs as a therapeutic target.

Materials and Methods

Study Approval and Human Subjects. All experiments involving mice were approved by the Animal Research Committee of Kyoto University and performed in accordance with Japanese government regulations. Surgically resected specimens were obtained from 57 CRC patients at Kyoto University Hospital. Analyses for human subjects were approved by the ethical committee of Kyoto University Hospital, and written informed consent was obtained from all subjects before inclusion in the study.

Details about animal models, organoid/spheroid culture, CRISPR-Cas9 genome editing of organoids, lentivirus transduction, siRNA transfection, xenotransplantation of organoids, immunostaining, evaluation of tuft cell-like cancer cells in hCRCs, time-lapse imaging, qRT-PCR, microarray analysis, flow cytometry, statistical analysis, and data availability are described in *SI Appendix, Materials and Methods*.

ACKNOWLEDGMENTS. We thank Kyoto University Live Imaging Center for technical support and all members of H.S. and A.F. laboratories for helpful suggestions. This work was supported in part by Grants-in-Aid KAKENHI (26293173, 15H06334, 16H06280, 16K09394, 16K15427, 17H04157, 16H06280 "ABiS"); Project for Cancer Research and Therapeutic Evolution (P-CREATE) from the Japan Agency for Medical Research and Development; the Kobayashi Foundation for Cancer Research; the Naito Foundation; Research Grant of the Princess Takamatsu Cancer Research Fund 13-24514; the Mitsubishi Foundation; the Takeda Science Foundation; Uehara Memorial Foundation; the Mochida Foundation; and the Pancreas Research Foundation of Japan.

1. E. Batlle, H. Clevers, Cancer stem cells revisited. *Nat. Med.* **23**, 1124–1134 (2017).
2. M. Shimokawa *et al.*, Visualization and targeting of LGR5$^+$ human colon cancer stem cells. *Nature* **545**, 187–192 (2017).
3. C. Cortina *et al.*, A genome editing approach to study cancer stem cells in human tumors. *EMBO Mol. Med.* **9**, 869–879 (2017).
4. N. Barker *et al.*, Identification of stem cells in small intestine and colon by marker gene Lgr5. *Nature* **449**, 1003–1007 (2007).
5. E. Sangiorgi, M. R. Capecchi, Bmi1 is expressed in vivo in intestinal stem cells. *Nat. Genet.* **40**, 915–920 (2008).
6. H. J. Snippert *et al.*, Prominin-1/CD133 marks stem cells and early progenitors in mouse small intestine. *Gastroenterology* **136**, 2187–2194.e1 (2009).
7. L. Zhu *et al.*, Prominin 1 marks intestinal stem cells that are susceptible to neoplastic transformation. *Nature* **457**, 603–607 (2009).
8. H. Tian *et al.*, A reserve stem cell population in small intestine renders Lgr5-positive cells dispensable. *Nature* **478**, 255–259 (2011).
9. F. de Sousa e Melo *et al.*, A distinct role for Lgr5$^+$ stem cells in primary and metastatic colon cancer. *Nature* **543**, 676–680 (2017).
10. Y. Nakanishi *et al.*, Dclk1 distinguishes between tumor and normal stem cells in the intestine. *Nat. Genet.* **45**, 98–103 (2013).
11. Y. Iwakura, H. Ishigame, S. Saijo, S. Nakae, Functional specialization of interleukin-17 family members. *Immunity* **34**, 149–162 (2011).
12. Y. Shi *et al.*, A novel cytokine receptor-ligand pair. Identification, molecular characterization, and in vivo immunomodulatory activity. *J. Biol. Chem.* **275**, 19167–19176 (2000).
13. F. Gerbe *et al.*, Intestinal epithelial tuft cells initiate type 2 mucosal immunity to helminth parasites. *Nature* **529**, 226–230 (2016).
14. M. R. Howitt *et al.*, Tuft cells, taste-chemosensory cells, orchestrate parasite type 2 immunity in the gut. *Science* **351**, 1329–1333 (2016).
15. J. von Moltke, M. Ji, H. E. Liang, R. M. Locksley, Tuft-cell-derived IL-25 regulates an intestinal ILC2-epithelial response circuit. *Nature* **529**, 221–225 (2016).
16. C. Schneider *et al.*, A metabolite-triggered tuft cell-ILC2 circuit drives small intestinal remodeling. *Cell* **174**, 271–284.e14 (2018).
17. J. M. Reynolds *et al.*, Interleukin-17B antagonizes interleukin-25-mediated mucosal inflammation. *Immunity* **42**, 692–703 (2015).
18. Y. Yamaga *et al.*, Gene expression profile of Dclk1(+) cells in intestinal tumors. *Dig. Liver Dis.* **50**, 1353–1361 (2018).
19. C. Bezençon *et al.*, Murine intestinal cells expressing Trpm5 are mostly brush cells and express markers of neuronal and inflammatory cells. *J. Comp. Neurol.* **509**, 514–525 (2008).
20. A. L. Haber *et al.*, A single-cell survey of the small intestinal epithelium. *Nature* **551**, 333–339 (2017).
21. H. H. Wu *et al.*, Targeting IL-17B-IL-17RB signaling with an anti-IL-17RB antibody blocks pancreatic cancer metastasis by silencing multiple chemokines. *J. Exp. Med.* **212**, 333–349 (2015).
22. S. Furuta *et al.*, IL-25 causes apoptosis of IL-25R-expressing breast cancer cells without toxicity to nonmalignant cells. *Sci. Transl. Med.* **3**, 78ra31 (2011).
23. D. R. Neill *et al.*, Nuocytes represent a new innate effector leukocyte that mediates type-2 immunity. *Nature* **464**, 1367–1370 (2010).
24. N. Harada *et al.*, Intestinal polyposis in mice with a dominant stable mutation of the beta-catenin gene. *EMBO J.* **18**, 5931–5942 (1999).
25. J. Muñoz *et al.*, The Lgr5 intestinal stem cell signature: Robust expression of proposed quiescent '+4' cell markers. *EMBO J.* **31**, 3079–3091 (2012).
26. A. H. Bild *et al.*, Oncogenic pathway signatures in human cancers as a guide to targeted therapies. *Nature* **439**, 353–357 (2006).
27. J. Lamb *et al.*, A mechanism of cyclin D1 action encoded in the patterns of gene expression in human cancer. *Cell* **114**, 323–334 (2003).
28. A. G. Schepers *et al.*, Lineage tracing reveals Lgr5+ stem cell activity in mouse intestinal adenomas. *Science* **337**, 730–735 (2012).
29. S. Schwitalla *et al.*, Intestinal tumorigenesis initiated by dedifferentiation and acquisition of stem-cell-like properties. *Cell* **152**, 25–38 (2013).
30. M. van der Heijden *et al.*, Bcl-2 is a critical mediator of intestinal transformation. *Nat. Commun.* **7**, 10916 (2016).
31. H. J. Snippert, A. G. Schepers, J. H. van Es, B. D. Simons, H. Clevers, Biased competition between Lgr5 intestinal stem cells driven by oncogenic mutation induces clonal expansion. *EMBO Rep.* **15**, 62–69 (2014).
32. H. Miyoshi *et al.*, An improved method for culturing patient-derived colorectal cancer spheroids. *Oncotarget* **9**, 21950–21964 (2018).
33. H. Maekawa *et al.*, A chemosensitivity study of colorectal cancer using xenografts of patient-derived tumor-initiating cells. *Mol. Cancer Ther.* **17**, 2187–2196 (2018).
34. F. Gerbe *et al.*, Distinct ATOH1 and Neurog3 requirements define tuft cells as a new secretory cell type in the intestinal epithelium. *J. Cell Biol.* **192**, 767–780 (2011).
35. J. F. Urban, , Jr, *et al.*, IL-13, IL-4Ralpha, and Stat6 are required for the expulsion of the gastrointestinal nematode parasite Nippostrongylus brasiliensis. *Immunity* **8**, 255–264 (1998).
36. Y. H. Huang *et al.*, POU2F3 is a master regulator of a tuft cell-like variant of small cell lung cancer. *Genes Dev.* **32**, 915–928 (2018).
37. T. Sato *et al.*, Single Lgr5 stem cells build crypt-villus structures in vitro without a mesenchymal niche. *Nature* **459**, 262–265 (2009).
38. C. K. Huang *et al.*, Autocrine/paracrine mechanism of interleukin-17B receptor promotes breast tumorigenesis through NF-κB-mediated antiapoptotic pathway. *Oncogene* **33**, 2968–2977 (2014).
39. S. C. Huang *et al.*, TGF-β1 secreted by Tregs in lymph nodes promotes breast cancer malignancy via up-regulation of IL-17RB. *EMBO Mol. Med.* **9**, 1660–1680 (2017).
40. M. R. Junttila *et al.*, Targeting LGR5+ cells with an antibody-drug conjugate for the treatment of colon cancer. *Sci. Transl. Med.* **7**, 314ra186 (2015).
41. M. Biton *et al.*, T helper cell cytokines modulate intestinal stem cell renewal and differentiation. *Cell* **175**, 1307–1320.e22 (2018).
42. J. R. McDermott, N. E. Humphreys, S. P. Forman, D. D. Donaldson, R. K. Grencis, Intraepithelial NK cell-derived IL-13 induces intestinal pathology associated with nematode infection. *J. Immunol.* **175**, 3207–3213 (2005).
43. R. L. Maywald *et al.*, IL-33 activates tumor stroma to promote intestinal polyposis. *Proc. Natl. Acad. Sci. U.S.A.* **112**, E2487–E2496 (2015).
44. E. R. Fearon, B. Vogelstein, A genetic model for colorectal tumorigenesis. *Cell* **61**, 759–767 (1990).